Title

Role of Marek's Disease Virus (MDV)-Encoded US3 Serine/Threonine Protein Kinase in Regulating MDV Meq and Cellular CREB Phosphorylation

Journal

Journal of Virology, 94(17)

ISSN

0022-538X

Authors

Liao, Yifei

Lupiani, Blanca

Bajwa, Kanika

et al.

Publication Date

2020-08-17

DOI

10.1128/jvi.00892-20

Peer reviewed

AMERICAN SOCIETY FOR MICROBIOLOGY | Journal of Virology®

VIRUS-CELL INTERACTIONS

Role of Marek's Disease Virus (MDV)-Encoded U_S3 Serine/Threonine Protein Kinase in Regulating MDV Meq and Cellular CREB Phosphorylation

Yifei Liao,[a] Blanca Lupiani,[a] Kanika Bajwa,[a] Owais A. Khan,[a] Yoshihiro Izumiya,[b] Sanjay M. Reddy[a]

[a]Department of Veterinary Pathobiology, College of Veterinary Medicine and Biomedical Sciences, Texas A&M University, College Station, Texas, USA
[b]Department of Dermatology, School of Medicine, University of California, Davis, Sacramento, California, USA

ABSTRACT Marek's disease (MD) is a neoplastic disease of chickens caused by Marek's disease virus (MDV), a member of the subfamily *Alphaherpesvirinae*. Like other alphaherpesviruses, MDV encodes a serine/threonine protein kinase, U_S3. The functions of U_S3 have been extensively studied in other alphaherpesviruses; however, the biological functions of MDV U_S3 and its substrates have not been studied in detail. In this study, we investigated potential cellular pathways that are regulated by MDV U_S3 and identified chicken CREB (chCREB) as a substrate of MDV U_S3. We show that wild-type MDV U_S3, but not kinase-dead U_S3 (U_S3-K220A), increases CREB phosphorylation, leading to recruitment of phospho-CREB (pCREB) to the promoter of the CREB-responsive gene and activation of CREB target gene expression. Using U_S3 deletion and U_S3 kinase-dead recombinant MDV, we identified U_S3-responsive MDV genes during infection and found that the majority of U_S3-responsive genes were located in the MDV repeat regions. Chromatin immunoprecipitation sequencing (ChIP-seq) studies determined that some U_S3-regulated genes colocalized with Meq (an MDV-encoded oncoprotein) recruitment sites. Chromatin immunoprecipitation-PCR (ChIP-PCR) further confirmed Meq binding to the *ICP4/LAT* region, which is also regulated by U_S3. Furthermore, biochemical studies demonstrated that MDV U_S3 interacts with Meq in transfected cells and MDV-infected chicken embryonic fibroblasts in a phosphorylation-dependent manner. Finally, *in vitro* kinase studies revealed that Meq is a U_S3 substrate. MDV U_S3 thus acts as an upstream kinase of the CREB signaling pathway to regulate the transcription function of the CREB/Meq heterodimer, which targets cellular and viral gene expression.

IMPORTANCE MDV is a potent oncogenic herpesvirus that induces T-cell lymphoma in infected chickens. Marek's disease continues to have a significant economic impact on the poultry industry worldwide. U_S3 encoded by alphaherpesviruses is a multifunctional kinase involved in the regulation of various cellular pathways. Using an MDV genome quantitative reverse transcriptase PCR (qRT-PCR) array and chromatin immunoprecipitation, we elucidated the role of MDV U_S3 in viral and cellular gene regulation. Our results provide insights into how viral kinase regulates host cell signaling pathways to activate both viral and host gene expression. This is an important step toward understanding host-pathogen interaction through activation of signaling cascades.

KEYWORDS CREB, Marek's disease virus, Meq, US3 protein kinase, herpesviruses, transcription regulation

Marek's disease (MD) is a highly contagious lymphoproliferative disease of chickens that was first described by József Marek in 1907 (1). Later, the causative agent of MD was identified as Marek's disease virus (MDV), which was classified as a member of

Citation Liao Y, Lupiani B, Bajwa K, Khan OA, Izumiya Y, Reddy SM. 2020. Role of Marek's disease virus (MDV)-encoded U_S3 serine/threonine protein kinase in regulating MDV Meq and cellular CREB phosphorylation. J Virol 94:e00892-20. https://doi.org/10.1128/JVI.00892-20.

Editor Jae U. Jung, University of Southern California

Address correspondence to Sanjay M. Reddy, SReddy@cvm.tamu.edu.

Received 8 May 2020
Accepted 15 June 2020
Accepted manuscript posted online 24 June 2020
Published 17 August 2020

the subfamily *Alphaherpesvirinae* based on DNA sequence homology and genome organization (2, 3). Infection of chickens with highly virulent strains of MDV results in the formation of T-cell lymphomas as early as 2 weeks postinfection (4). Three MDV serotypes have been identified and their genomes sequenced: MDV-1 (*Gallid alphaherpesvirus* type 2 [GaHV-2]), which includes oncogenic MDV and its cell-culture-attenuated variants; MDV-2 (GaHV-3), which includes the naturally nononcogenic MDV; and turkey herpesvirus (HVT) (*Meleagrid alphaherpesvirus* type 1 [MeHV-1]) (1, 5). Similar to other alphaherpesviruses, the 160- to 180-kb double-stranded DNA genome of MDV, which encodes more than 100 putative genes, consists of a long (U_L) and a short (U_S) unique region, each flanked by inverted repeats (TR_L, IR_L, IR_S, and TR_S) (6, 7). Two genes, *meq* and *vTR*, within the TR_L and IR_L regions have been shown to be directly involved in MDV lymphomagenesis (8, 9).

MDV (MDV refers to MDV-1 below unless otherwise specified)-encoded U_S3 protein is a serine/threonine protein kinase that is highly conserved among all alphaherpesviruses. U_S3 contains a kinase activity domain consisting of an ATP-binding domain and a catalytic active site, which is important for its kinase activity (10). The functions of U_S3 have been extensively explored in herpes simplex virus 1 (HSV-1). Although it is not essential for virus growth *in vitro*, multiple functions have been attributed to U_S3, including transcription regulation, cytoskeletal rearrangements, antiapoptosis, and interference with the interferon (IFN) system (10). In addition, HSV-1 U_S3 shuttles between the nucleus and the cytoplasm, and the kinase activity is important for its subcellular localization (10, 11). In addition to autophosphorylation, several cellular and viral proteins have been identified as U_S3 substrates. HSV-1 U_S3 protein substrates include U_L31, U_L34, and glycoprotein B (gB) (12, 13). Cellular proteins, such as p65, histone deacetylase 1 (HDAC-1) and HDAC-2, programmed cell death protein 4 (PDCD4), and cAMP response element-binding protein (CREB), are also substrates of HSV-1 U_S3 (11, 14–16). It has been reported that MDV U_S3 is involved in actin stress fiber breakdown and is important for de-envelopment of perinuclear virions (17). In addition, MDV pp38 protein was identified as a substrate and interaction partner of MDV U_S3, and MDV U_S3 was shown to be important for protecting cells from apoptosis in a kinase activity-dependent manner (18, 19).

MDV encodes a 339-amino-acid-long b-ZIP protein called Meq, which consists of an N-terminal DNA binding domain, a leucine zipper domain, and a C-terminal transactivation/transrepression domain (8). Meq is expressed both during the lytic infection phase and in lymphoblastoid tumor cells (20), and deletion of both copies of the *meq* gene from the MDV genome results in the absence of tumors in infected chickens, indicating that Meq is essential for transformation of lymphocytes (8). Meq has been identified as a homolog of the Jun-Fos family of transcription factors. Through the leucine zipper region, Meq forms homodimers with itself and heterodimers with cellular c-Jun and c-Fos (21, 22), which bind to specific DNA sequences, called Meq-responsive element I (MERE I) and MERE II, respectively (23). In addition, a chromatin immunoprecipitation (ChIP) study showed that Meq directly binds to the MDV lytic origin of replication and Meq and ICP4 promoters (24). Further, application of advanced high-throughput technologies, such as microarray and next-generation sequencing, provided a comprehensive view of Meq binding sites within the chicken genome and the role of Meq in regulating cellular pathways, including ERK/MAPK, Jak-STAT, and ErbB pathways (25).

CREB is a transcription factor that binds as a dimer to the conserved cAMP response element (CRE), TGACGTCA (26, 27). CREB is highly conserved between humans and chickens and can form heterodimers with MDV Meq (24). Phosphorylation of CREB at serine 133 (S133) by various cellular protein kinases, such as PKA, calmodulin-depend ent kinase (CaMK) IV, and MAPK-activated ribosomal S6 kinases (RSKs), activates CREB, resulting in the recruitment of CREB-binding protein (CBP)/p300 to the promoters of CREB target genes to further affect the chromatin structure, enabling synthesis of RNA by RNA polymerase II (26, 28). HSV-1 U_S3 has been shown to phosphorylate endog enous and cotransfected CREB at S133 (16). Studies of several herpesviruses suggest

that activation of CREB plays an important role in herpesvirus infection. Kaposi's sarcoma-associated herpesvirus (KSHV) utilizes multiple cellular signal pathways to activate CREB to regulate expression of cyclooxygenase 2 (COX-2), a host factor that plays an important role in KSHV latency and pathogenesis (29). Another recent study showed that varicella-zoster virus (VZV) infection upregulates CREB phosphorylation, which does not require VZV-encoded serine/threonine protein kinases, and the intera ction between phospho-CREB (pCREB) and CBP/p300 is important for skin infection by VZV (30). In addition, other studies showed that activation of CBP/p300 plays an important role in regulating herpesvirus reactivation from latency (31, 32).

In this study, we aimed to identify MDV U_S3 viral and cellular substrates and to investigate the role of MDV U_S3 in regulating MDV-host interaction. Our results show that MDV U_S3 interacts with and phosphorylates MDV Meq and chicken CREB (chCREB). Further, quantitative reverse transcriptase PCR (qRT-PCR) and ChIP experiments showed that MDV U_S3 enhances enrichment of pCREB at the promoter of CREB target genes to upregulate their expression, and MDV U_S3 is important for the expression of several MDV genes during infection. Overall, our studies point to a role for MDV U_S3 in transcriptional regulation of both host and viral genes during MDV infection.

RESULTS

MDV U_S3 and chCREB transactivate CRE in a luciferase reporter assay. To identify the biological function of MDV U_S3, we first explored possible signaling pathways regulated by U_S3. We utilized signaling reporter systems that examined specific transcription factor activity, as each reporter construct encodes tandem specific DNA-responsive elements for the transcriptional factor (e.g., STAT3 and CREB) (Fig. 1A). We tested a total of 29 reporter constructs and found that MDV U_S3 strongly induces luciferase expression from several reporter constructs, including CREB, KLF4, ATF6, HNF4, and PPAR (Fig. 1A). Among them, the CREB pathway showed the highest activation after transfection with an MDV U_S3 expression plasmid. More importantly, the activation was found to be kinase dependent, as transient expression of an MDV U_S3 kinase-dead mutant (U_S3-K220A) did not activate the CREB reporter construct (Fig. 1B). We also found that phosphorylation of S119 of chCREB (corresponding to S133 of human CREB [hCREB]) is important for this transactivation activity (Fig. 1C). Furthermore, transfection of cells with chCREB_S119D (a phosphorylation mimic form) resulted in higher levels of CRE-responsive-element transactivation, while chCREB_S119A (a nonphosphorylated form) showed lower levels of transactivation.

MDV U_S3 increases phosphorylation of CREB. To explore the role of MDV U_S3 in regulating CREB phosphorylation, levels of pCREB were examined in pcDNA-FLAG-U_S3 (wild type; FLAG-U_S3) plasmid-, pcDNA-FLAG-U_S3-K220A (kinase dead; FLAG-U_S3-K220A) plasmid-, or pcDNA empty-vector (Ev) plasmid-transfected 293T cells. Forty-eight hours after transfection, total cell lysates were subjected to sodium dodecyl sulfate-polyacrylamide gel electrophoresis (SDS-PAGE) and Western blot (WB) analysis with pCREB antibody that specifically recognizes hCREB serine133 phosphorylation (corresponding to chCREB serine 119) (Fig. 2E). As shown in Fig. 2A, left, expression of FLAG-U_S3, but not FLAG-U_S3-K220A, increased the levels of pCREB. Quantification of the WB results showed that the pCREB/total CREB (tCREB) ratio in pcDNA-FLAG-U_S3-transfected cells was about 1.7-fold higher than in pcDNA-FLAG-U_S3-K220A-transfected cells and about 1.3-fold higher than in pcDNA Ev-transfected cells (Fig. 2A, right). In addition, the pCREB/tCREB ratio in pcDNA-FLAG-U_S3-K220A-transfected cells was slightly lower than in pcDNA Ev-transfected cells, which may be due to competition between kinase-dead U_S3 and other cellular protein kinases (33, 34). These results were confirmed by cotransfecting pcDNA-hCREB or pcDNA-chCREB with pcDNA-FLAG-U_S3, pcDNA-FLAG-U_S3-K220A, or pcDNA Ev into 293T (Fig. 2B) and DF-1 (Fig. 2C) cells, respectively. WB analysis and quantification confirmed that overexpression of MDV U_S3 clearly increased the pCREB/tCREB ratio (3- to 4-fold) compared to U_S3-K220A or Ev in cotransfected cells. To further examine the role of U_S3 in regulating CREB phosphorylation during natural infection, we analyzed pCREB levels in MDV-infected chicken

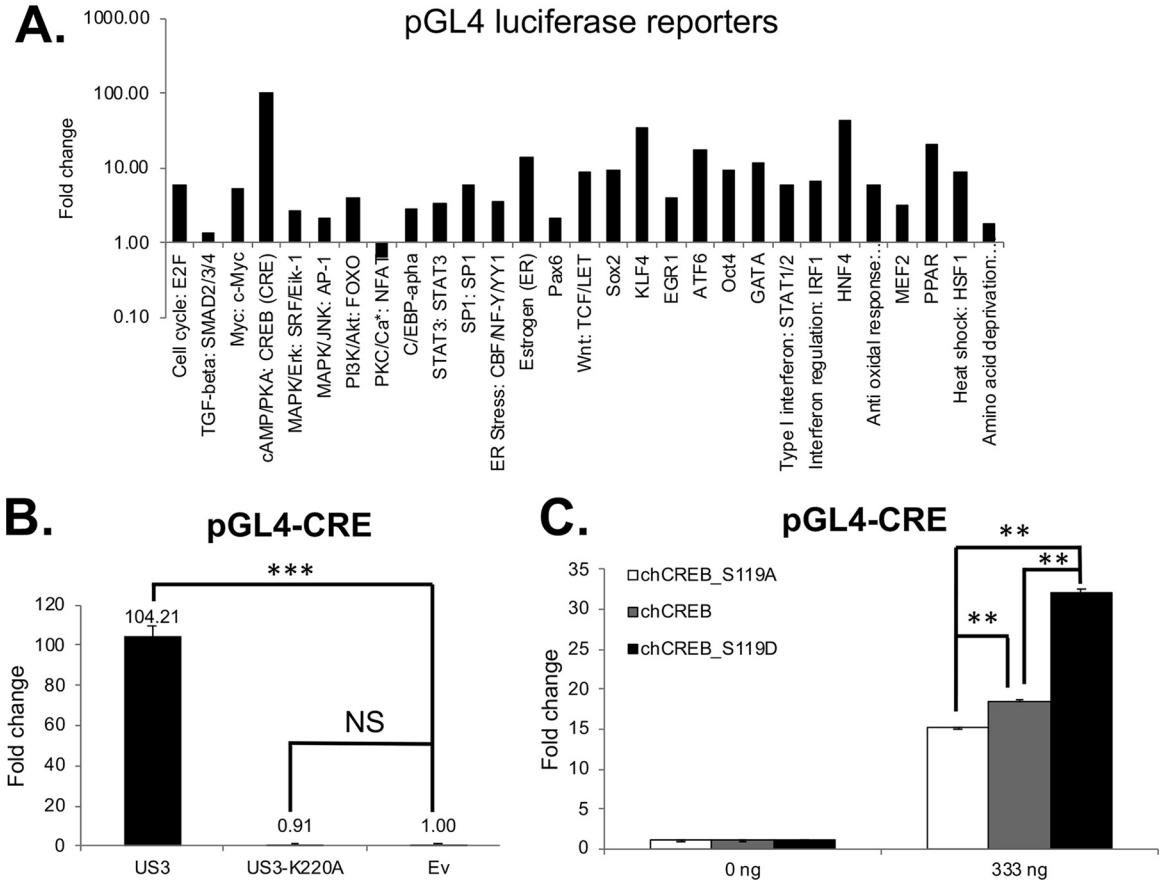

FIG 1 MDV U_S3 and chCREB transactivate CRE in a luciferase reporter assay. (A) pcDNA-U_S3 or pcDNA Ev was cotransfected with the indicated luciferase reporter plasmids. Firefly luciferase was measured 48 h posttransfection. The data are presented as fold change relative to Ev. (B) pcDNA-U_S3, pcDNA-U_S3-K220A, or pcDNA Ev was cotransfected with the pGL4-CRE reporter vector and the *Renilla* luciferase vector into 293T cells. Forty-eight hours after transfection, firefly luciferase and *Renillla* luciferase activities were measured using the Dual-Glo luciferase assay system according to the manufacturer's protocol. The numbers above the bars indicate the fold change relative to Ev. (C) 293T cells were cotransfected with different amounts of pcDNA-chCREB_S119A, pcDNA-chCREB, and pcDNA-chCREB_S119D with the pGL4-CRE reporter vector and the *Renilla* luciferase vector. A dual-luciferase assay was performed as described above. The experiment was repeated three times in triplicate. The error bars indicate standard errors of the mean (SEM). NS, not significant; **, $P < 0.01$; ***, $P < 0.001$.

embryonic fibroblasts (CEF). As shown in Fig. 2D, pCREB levels were higher in 686-BAC parental-virus-infected CEF than in noninfected CEF, while pCREB levels in 686-BACΔU_S3 (U_S3-null virus)-infected CEF were slightly lower than in noninfected CEF, in agreement with transfection experiments (Fig. 2A). MDV pp38 phosphorylation was used as a control to demonstrate the effects of U_S3 deletion in 686-BACΔU_S3 virus (Fig. 2D). Because U_S3 kinases of all three MDV serotypes present a conserved catalytic active site (see Fig. S1A in the supplemental material), we examined if the ability to phosphorylate CREB was conserved in all three serotypes. Similar to MDV, MDV-2 and HVT U_S3 kinases also increased the levels of pCREB/tCREB in transfection studies (see Fig. S1B and C).

Overexpression of MDV U_S3 enhances enrichment of pCREB at the promoter of c-*Fos* to upregulate its expression. To examine the role of U_S3-mediated CREB phosphorylation in gene regulation, we performed qRT-PCR of c-*Fos*, a CREB target gene, which also forms heterodimers with MDV Meq (24, 35). Because of the high reproducibility and high efficiency of transient transfection, we carried out these experiments in 293T cells. Transient expression of MDV U_S3 in 293T cells increased the expression of c-*Fos* compared to U_S3-K220A and Ev (Fig. 3A). Interestingly, compared to Ev, expression of U_S3-K220A inhibited expression of c-*Fos* (Fig. 3A). Similar results were observed when pcDNA-U_S3 of MDV-2 and HVT were transfected (see Fig. S1D). To

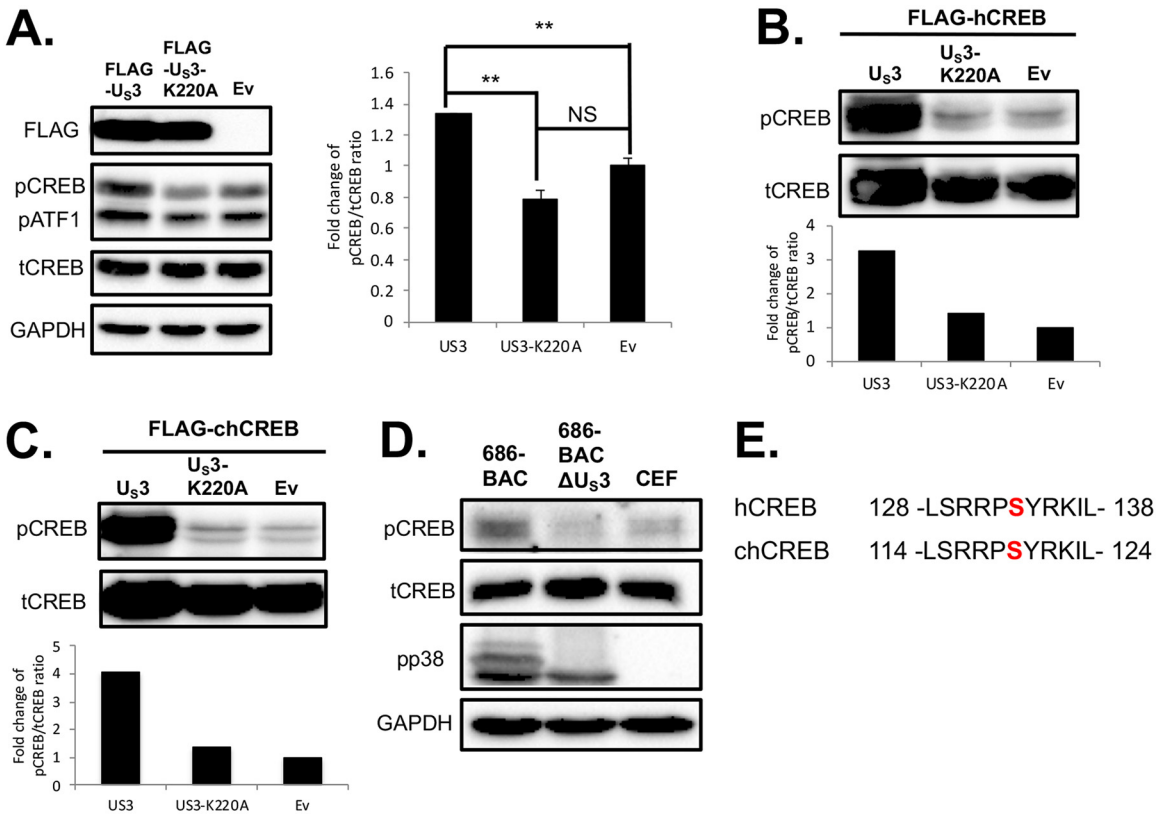

FIG 2 MDV U_S3 increases phosphorylation of CREB. (A) pcDNA-FLAG-U_S3, pcDNA-FLAG-U_S3-K220A, or pcDNA Ev was transfected into 293T cells. (Left) The cells were lysed 48 h posttransfection, followed by WB analysis with the indicated antibodies. Representative data from three independent cell culture experiments. (Right) The pCREB/tCREB ratio was quantified with Image J software and is presented as the fold change compared to Ev; *t* tests were performed between groups. **, $P < 0.01$; NS, not significant. (B and C) 293T cells (B) and DF-1 cells (C) were cotransfected with the indicated plasmids. Forty-eight hours after transfection, the cells were lysed and subjected to SDS-PAGE and WB with the indicated antibodies. (Top) WB results. (Bottom) Fold change in the pCREB/tCREB ratio. (D) CEF were infected with 686-BAC or 686-BACΔU_S3 virus. Seven days after infection, the cells were lysed and subjected to SDS-PAGE and WB with the indicated antibodies. (E) Amino acid sequence alignment of a major phosphorylation subdomain of hCREB and chCREB proteins. The serine residue detected by pCREB antibody is shown in red. The numbers indicate amino acid locations, and the dashes represent amino acids not shown in the alignment.

further confirm our results in chicken cells, we repeated the same experiment in chicken DF-1 cells. Our results showed that transfection of pcDNA-U_S3 increased the mRNA level of c-*Fos* in DF-1 cells, but transfection of pcDNA-U_S3-K220A had no effect on c-*Fos* expression compared to pcDNA Ev (Fig. 3B). These results suggest that MDV U_S3 could activate CREB target gene expression, presumably through induction of CREB phosphorylation.

As shown above, our results show that MDV U_S3 increases phosphorylation of CREB and upregulates expression of a CREB target gene. In order to prove if U_S3 is responsible for activation of pCREB and c-*Fos* expression, we examined MDV U_S3-dependent pCREB recruitment to the c-*Fos* promoter. To study this, 293T cells (Fig. 3C) or DF-1 cells (Fig. 3D) were cotransfected with pcDNA-U_S3, pcDNA-U_S3-K220A, or pcDNA Ev with pcDNA-hCREB or pcDNA-chCREB. Forty-eight hours posttransfection, the cells were fixed and subjected to ChIP assay with pCREB antibody and normal IgG, followed by qPCR analysis of the c-*Fos* promoter, as previously reported (36, 37). As shown in Fig. 3C, compared to U_S3-K220A (gray bars) or Ev (black bars), overexpression of wild-type U_S3 (white bars) consistently increased the enrichment of pCREB at the c-*Fos* promoter but not at the c-*Fos* coding region, used as a negative control (c-Fos_Ng). In addition, the enrichment of pCREB at the human c-*Fos* promoter was significantly lower in pcDNA-U_S3-K220A-transfected cells than in pcDNA Ev-transfected cells; these results are consistent with the above-mentioned qRT-PCR results, in which overexpression of

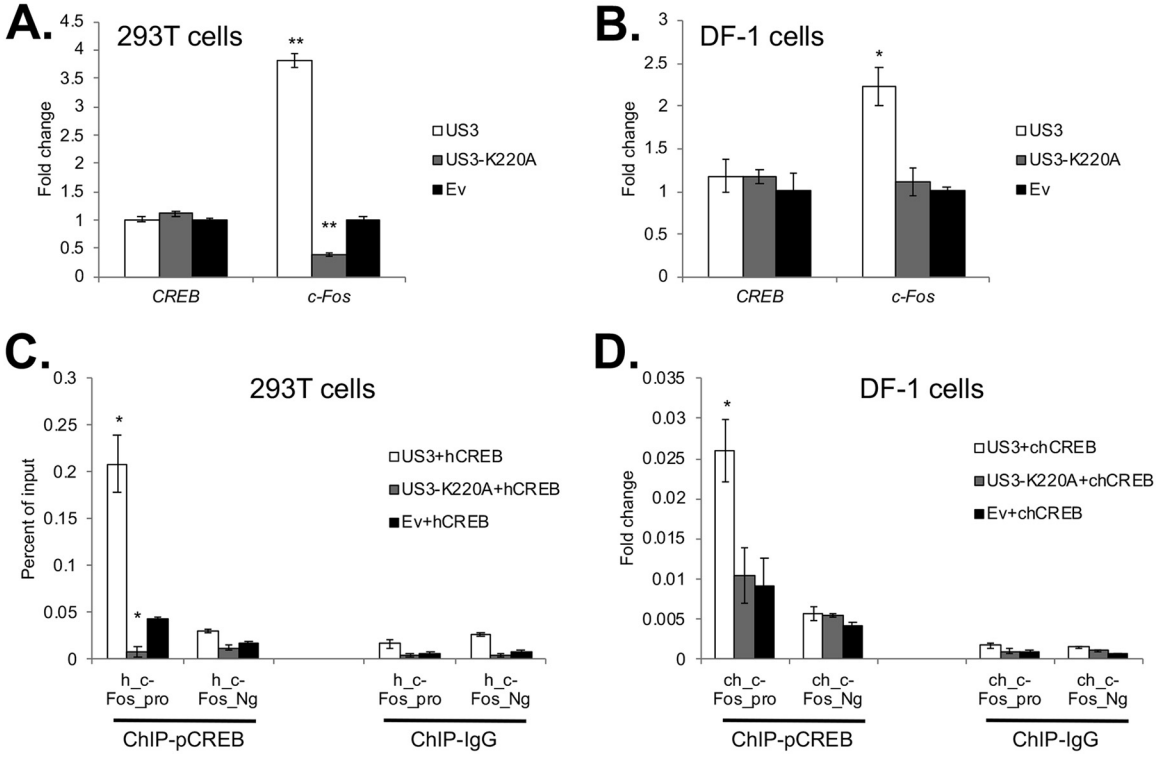

FIG 3 Overexpression of MDV U_S3 enhances enrichment of pCREB at the c-*Fos* promoter to upregulate its expression. (A and B) 293T cells (A) or DF-1 cells (B) were transfected with pcDNA-U_S3, pcDNA-U_S3-K220A, or pcDNA Ev. Forty-eight hours after transfection, cells were harvested for RNA isolation, followed by cDNA synthesis and qRT-PCR analysis for c-*Fos*. The qRT-PCR data were analyzed using the $2^{-\Delta\Delta CT}$ method. Human GAPDH or chicken GAPDH was used as an internal control. The data represent averages ± standard deviations of the results of three independent experiments. The data are presented as the fold change relative to Ev. (C and D) 293T cells were cotransfected with pcDNA-U_S3, pcDNA-U_S3-K220A, or pcDNA Ev and pcDNA-hCREB (C) or pcDNA-chCREB (D). Forty-eight hours after transfection, the cells were fixed with formaldehyde solution and subjected to ChIP assay with rabbit anti-pCREB antibody (left) or normal rabbit IgG antibody (right), followed by qPCR analysis with the indicated primers. ChIP enrichment signals were normalized to those derived from an input DNA control. pro, promoter; Ng, negative control. *, $P < 0.05$; **, $P < 0.01$.

U_S3-K220A significantly decreased mRNA levels of the human c-*Fos* gene (Fig. 3A). Similar experiments were also performed in DF-1 cells. As shown in Fig. 3D, the promoter of chicken c-*Fos* was highly occupied by pCREB in pcDNA-U_S3- and pcDNA-chCREB-cotransfected cells. Consistent with the DF-1 qRT-PCR results (Fig. 3B), expression of U_S3-K220A did not affect the occupation of pCREB at the chicken c-*Fos* promoter. These data suggest that MDV U_S3 upregulates the expression of CREB target genes by enhancing pCREB levels and further increasing the recruitment of pCREB to target promoters.

MDV U_S3 is important for the expression of several MDV genes. In addition to cellular genes, we next performed qRT-PCR with primers specific for 91 MDV genes to determine if MDV U_S3 plays a role in viral gene expression during infection. To examine the role of U_S3 expression and its kinase activity in regulating viral gene expression in naturally infected cells, CEF were infected with the same number of PFU of 686-BAC (parental), 686-BACΔU_S3 (U_S3 null), or 686-BAC_U_S3-K220A (U_S3 kinase-dead) viruses. The growth kinetics of these viruses were first determined by viral genome copy numbers. As reported previously (18), deletion of U_S3 or the U_S3 kinase-dead mutant reduced the replication of MDV compared to the parental virus (Fig. 4B). Seven days after infection with 686-BAC, 686-BACΔU_S3, or 686-BAC_U_S3-K220A virus, cells were harvested for RNA isolation and cDNA synthesis. MDV gene expression analysis was performed by qRT-PCR, and the results are shown as a heat map in Fig. 4A, where red indicates upregulation and green indicates downregulation. Deletion of U_S3 significantly upregulated 15 MDV genes and downregulated 19 MDV genes, while inactivation of U_S3 kinase activity significantly upregulated 14 MDV genes and downregulated

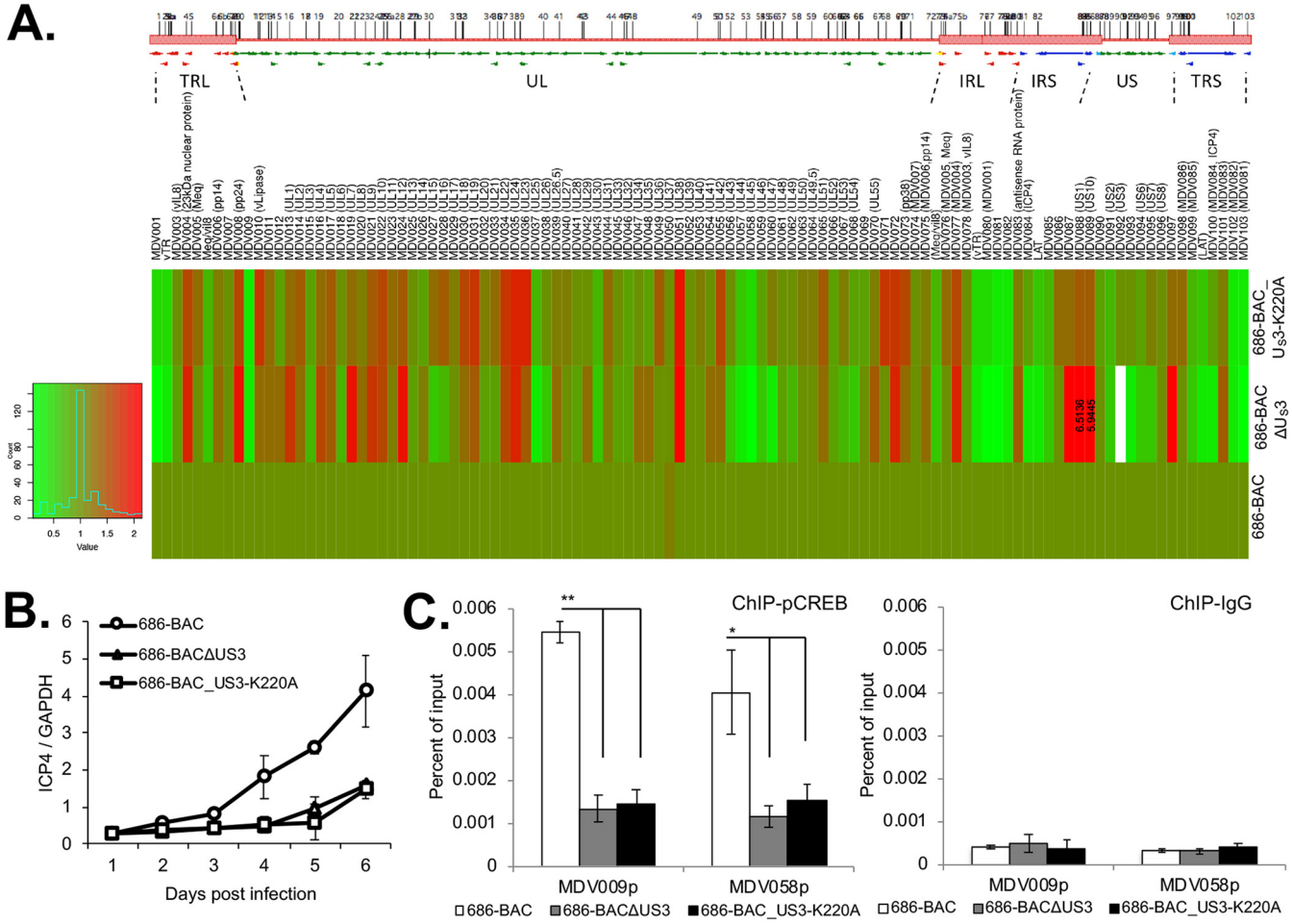

FIG 4 MDV U_S3 is important for viral gene expression. CEF were infected with 686-BAC, 686-BACΔU_S3, or 686-BAC-U_S3-K220A virus. (A) Seven days after infection, cells were harvested for RNA isolation. RNA was used for cDNA synthesis, followed by qRT-PCR analysis with the indicated gene primers. The qRT-PCR data were analyzed using the $2^{-\Delta\Delta CT}$ method. Chicken GAPDH was used as an internal control. The heat map presents qRT-PCR analysis data as the fold change of each studied gene; red indicates upregulation, and green indicates downregulation. To better present the data, *MDV088* and *MDV089* are marked as outliers and labeled with the fold change in the heat map. An ORF map indicating the locations of MDV genes within the MDV genome is shown above the heat map. (B) Cells were harvested for DNA isolation daily after infection. The genome copy numbers of 686-BAC, 686-BACΔU_S3, and 686-BAC-U_S3-K220A viruses were measured by qPCR. (C) Seven days after infection, cells were fixed with formaldehyde solution and subjected to ChIP with rabbit anti-pCREB antibody (left) or normal rabbit IgG antibody (right), followed by qPCR analysis with the indicated primers. ChIP enrichment values were normalized to those derived from an input DNA control. *, $P < 0.05$; **, $P < 0.01$. The error bars indicate standard deviations (SD).

10 MDV genes. In total, 16 MDV genes were regulated differently upon infection with 686-BACΔU_S3 and 686-BAC_U_S3-K220A viruses; we speculate that these differences might be due to a kinase-independent function of U_S3. The promoters of highly downregulated genes (*MDV009* and *MDV058*) that responded to both 686-BACΔU_S3 and 686-BAC_U_S3-K220A viruses were cloned into pGL3, a luciferase reporter vector. A dual-luciferase assay was performed to investigate the roles of U_S3 and chCREB in regulating the transcription activities of these promoters. The transcriptional activities of the *MDV009* promoter (MDV009p) and the *MDV058* promoter (MDV058p) were upregulated in pcDNA-U_S3-transfected cells (purple bar), as well as pcDNA-U_S3 and pcDNA-chCREB-cotransfected cells (blue bar) (see Fig. S2A in the supplemental material). Further, a ChIP assay with pCREB antibody was performed with 686-BAC, 686-BACΔU_S3, and 686-BAC_U_S3-K220A virus-infected cells. Our qPCR results showed that enrichment of pCREB at the *MDV009* and *MDV058* promoters was significantly higher in 686-BAC than in 686-BACΔU_S3 and 686-BAC_U_S3-K220A viral genomes (Fig. 4C), indicating that U_S3 phosphorylates and activates chCREB to upregulate expression of both the *MDV009* and *MDV058* genes.

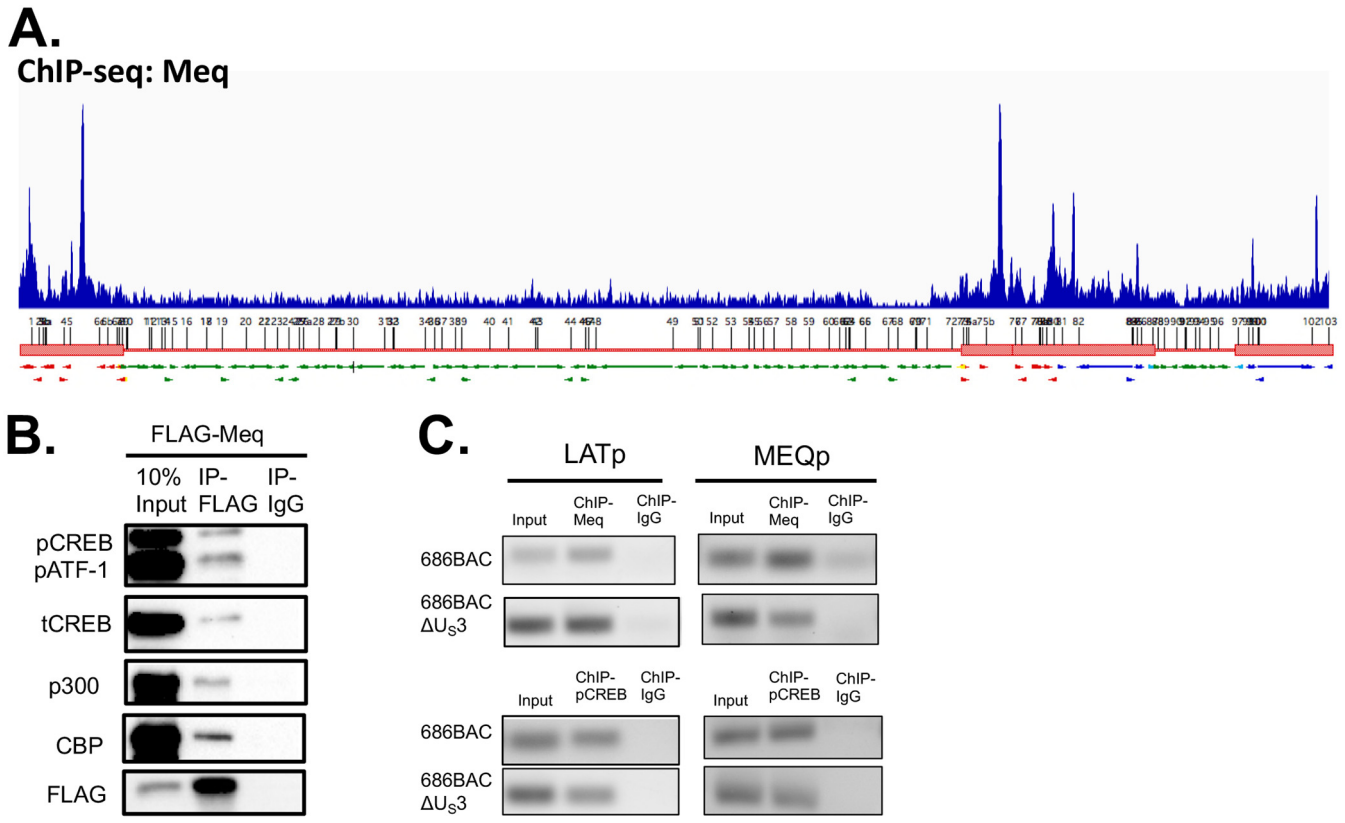

FIG 5 Corecruitment of MDV Meq and chCREB to viral promoters. (A) ChIP-seq analysis of Meq binding to the MDV genome. ChIP enrichment signals were normalized to those derived from an input DNA control. (B) 293T cells were transfected with pcDNA-FLAG-Meq. Forty-eight hours after transfection, 500 μg total cell lysates was used for IP with mouse anti-FLAG antibody or normal mouse IgG. WB was performed with the indicated antibodies. (C) CEF were infected with 686-BAC or 686-BACΔU_S3 virus. Seven days after infection, the cells were fixed and subjected to ChIP with rabbit anti-Meq antibody, rabbit anti-pCREB antibody, or normal rabbit IgG antibody. ChIP-PCRs were performed with the indicated primers.

Corecruitment of MDV Meq and chCREB proteins to viral promoters. A previous study by Levy et al. (24) showed that Meq forms dimers with CREB. In addition, they showed that CREB target genes closely align with Meq recruitment sites on the MDV genome (24). To confirm a potential association among Meq, U_S3, and CREB, we first determined Meq recruitment sites on the MDV genome using ChIP sequencing (ChIP-seq) analysis. Our results clearly demonstrate that Meq recruitment sites are largely enriched in both repeat regions of the genome, more specifically the *meq* and *ICP4/LAT* (Fig. 5A) regions. As expected from reported studies, Meq indeed formed a protein complex with CREB, as well as its coactivators, CBP/p300, in transfected cells (Fig. 5B). In addition, ChIP-PCR analysis demonstrated that Meq and chCREB are corecruited to the *LAT* (LATp) and *meq* (MEQp) promoters independently of U_S3-induced phosphorylation, while for MDV009p and MDV058p, recruitment of pCREB is enhanced in the presence of U_S3 (Fig. 5C; see Fig. S2B). Further, luciferase assay studies indicated that Meq cooperates with chCREB to activate viral promoters (see Fig. S2C) and CRE (see Fig. S2D).

MDV U_S3 interacts with and phosphorylates Meq. Next, we examined the physical association between MDV U_S3 and Meq proteins. Interestingly, our results show that Meq was efficiently coprecipitated by FLAG-U_S3, while it was only weakly associated with FLAG-U_S3-K220A; these results suggest that the kinase activity of U_S3 is important for its interaction with Meq (Fig. 6A). In addition, our immunofluorescence assay (IFA) results showed that Meq colocalizes with both wild-type U_S3 and U_S3-K220A in cell nuclei (see Fig. S3 in the supplemental material). The interaction between U_S3 and Meq was also examined in CEF infected with a recombinant 686-BAC virus containing C-terminally FLAG-tagged U_S3 (686-BAC-U_S3FLAG). Seven days after infec-

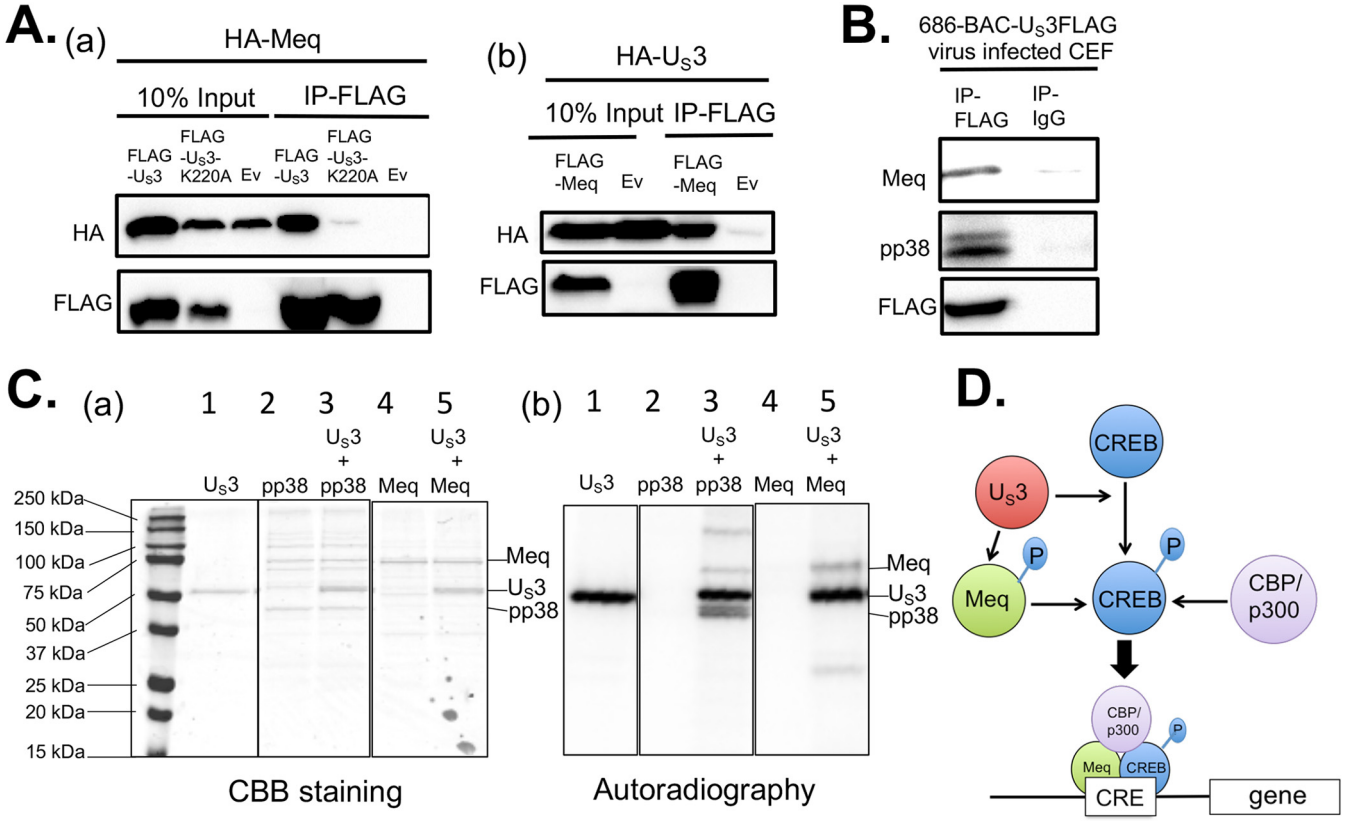

FIG 6 MDV U_S3 interacts with and phosphorylates Meq. (A) 293T cells were transfected with the indicated plasmids. Forty-eight hours after transfection, the cells were lysed and subjected to IP with anti-FLAG agarose beads, followed by WB with rabbit anti-HA antibody and rabbit anti-FLAG antibody. (B) CEF infected with 686-BAC-U_S3FLAG virus were lysed 7 days later and subjected to IP with mouse anti-FLAG antibody or normal mouse IgG. WB was performed with rabbit anti-Meq antibody, mouse anti-pp38 antibody, and rabbit anti-FLAG antibody. (C) Purified U_S3, Meq, and pp38 proteins were subjected to *in vitro* kinase assay, followed by CBB staining (a) and autoradiography (b). (D) Schematic representation of the roles of U_S3, Meq, CREB, and CBP/p300 in regulating gene expression. MDV Meq cooperates with pCREB-CBP/p300 complexes to activate gene expression.

tion with 686-BAC-U_S3FLAG, CEF were lysed in lysis buffer, followed by immunoprecipitation (IP) with FLAG antibody or with normal IgG as a negative control. A previous study showed that MDV U_S3 interacts with MDV pp38 protein (18), and we used this interaction as a control. As shown in Fig. 6B, both Meq and pp38 were coprecipitated by U_S3 protein in IP with FLAG antibody, but not with normal IgG.

Finally, *in vitro* kinase assays showed that, similar to other U_S3 protein kinases encoded by other alphaherpesviruses (38, 39), MDV U_S3 exhibits autophosphorylation activity (Fig. 6C, b, lanes 1, 3, and 5). In addition, in the presence of U_S3, both pp38 (Fig. 6C, b, lane 3) and Meq (Fig. 6C, b, lane 5) are phosphorylated compared to reactions without U_S3 (Fig. 6C, b, lanes 2 and 4). Total proteins were stained with Coomassie brilliant blue (CBB) (Fig. 6C, a). Taken together, these results suggest that MDV U_S3 protein associates with and phosphorylates Meq. A proposed model of the roles of U_S3, Meq, and CREB in regulating gene expression is illustrated in Fig. 6D.

DISCUSSION

Posttranslational modifications, such as methylation, phosphorylation, ubiquitylation, and SUMOylation, play important roles in regulating target protein functions, including gene regulation, protein stability, and protein-protein interactions (40). Among such modifications, phosphorylation, which affects a variety of viral and cellular processes, is one of the most common and extensively studied.

Previous reports indicated that alphaherpesvirus-encoded U_S3 serine/threonine protein kinase is a multifunctional protein that is involved in virus replication, virion morphogenesis, viral and cellular gene expression regulation, actin cytoskeleton re-

modeling, and antiapoptosis (10). U_S3 proteins of all alphaherpesviruses contain a highly conserved ATP-binding domain and a catalytic active site, even though overall U_S3 amino acid sequence similarity varies among different alphaherpesviruses. Among them, the substrates and functions of HSV-1 U_S3 have been widely explored. HSV-1 U_S3 phosphorylates viral proteins, including UL31, UL34, gB, and dUTPase (12, 13, 41), and cellular proteins, such as p65, HDAC-1, HDAC-2, PDCD4, CREB, interferon regulatory factor 3 (IRF3), and the cellular motor protein KIF3A (11, 14, 15, 42, 43). Initial characterization of MDV-encoded U_S3 showed that MDV U_S3 is not essential for virus growth in cell culture, although U_S3-null virus and U_S3 kinase-dead virus induced smaller plaques and exhibited reduced growth rates in infected CEF compared to the parental virus (17, 18).

To study the role of MDV U_S3, we first performed a series of luciferase assays to explore the cellular signaling pathways in which U_S3 is involved. The reporter vector pGL4-CRE was highly responsive to expression of MDV U_S3. A few other signaling pathways, including KLF4, ATF6, HNF4, and PPAR, were also responsive to U_S3 overexpression (Fig. 1). Cellular kinases target multiple other cellular kinases for cross talk; therefore, U_S3 may activate one or more cellular kinases, which may be responsible for multiple downstream signal activations detected in our screening. Future proteomics studies may comprehensively reveal U_S3 direct and indirect substrates. Nonetheless, we were able to demonstrate that overexpression of MDV U_S3 enhanced phosphorylation of CREB (Fig. 2), although we currently do not know if U_S3 directly or indirectly phosphorylates CREB. CREB responds to multiple stimuli, such as growth factors, peptide hormones, and $Ca2^+$ influx, and CREB activates a diverse array of target genes that are important for cell proliferation and differentiation and neuronal development (26, 44). Since CREB is phosphorylated by various cellular kinases, the exact mechanisms utilized by MDV U_S3 to increase CREB phosphorylation remain to be elucidated. Importantly, the ability of MDV U_S3 to induce CREB phosphorylation is conserved among all three MDV serotypes (see Fig. S1), despite relatively low sequence identity between MDV U_S3 and MDV-2 (59%) or HVT (60%) U_S3. Induction of MDV U_S3-mediated CREB phosphorylation increases the recruitment of pCREB to the c-*Fos* promoter, resulting in activation of c-*Fos* expression (Fig. 3) and indicating that MDV U_S3 alone can modulate cellular signaling pathways through activation of CREB.

Taking advantages of a well-established two-step Red-mediated recombination system, we generated MDV U_S3 deletion (686-BACΔU_S3) and U_S3-K220A kinase-dead (686-BAC_U_S3-K220A) mutant viruses. Infection of cells with 686-BACΔU_S3 and 686-BAC_U_S3-K220A mutant viruses in combination with a newly established MDV qPCR array revealed that MDV U_S3 is involved in the regulation of 34 MDV genes and that kinase activity of U_S3 is important for the expression of 24 MDV genes (Fig. 4). The existence of genes differentially regulated upon infection with 686-BACΔU_S3 and 686-BAC_U_S3-K220A viruses suggests that U_S3 may have kinase-independent activities that are involved in regulating viral gene expression. Among these MDV U_S3-activated genes, the *MDV009* (uncharacterized gene 9 protein) and *MDV058* (UL45) promoters of MDV 686-BAC have significantly higher occupancy of pCREB than MDV 686-BACΔU_S3 and 686-BAC_U_S3-K220A viruses (Fig. 4). Using the online promoter analysis tool PROMO (http://alggen.lsi.upc.es/cgi-bin/promo_v3/promo/promoinit.cgi?dirDB=TF_8.3), we could not find the full-length CRE motif (TGACGTCA) in these promoters. Instead, we found some predicted c-Jun and c-Fos binding sites, which are also the MDV Meq binding motif. In addition, previous work showed that only 26% of CREB binding sites contain full length CRE (45). We speculate that pCREB might be recruited to these promoters through the nonconsensus motif by Meq or other bZIP factors. In addition, it is interesting that most of the open reading frames (ORFs) located in IR_S/TR_S were dramatically downregulated by deletion of U_S3. This is supported by RNA sequencing (RNA-seq) studies with chicken T-cell lymphomas, which showed that these regions are transcriptionally highly active (data not shown) and also have multiple Meq binding sites (24).

We speculate that Meq and CREB coregulate these genomic regions, as our ChIP-seq

TABLE 1 Primers used in mutagenesis of MDV 686-BAC

Primer	Sequence (5′ to 3′)[a]
U_S3-Kan-F	TTATACTCTGGTAGAATATGAAACAGGGTTAAAACTAGGTAATAGACTGGAGGATGACGACGATAAGTAGGG
U_S3-Kan-R	TAGTATATATTATAAAATGAATCATTGAAGTTATTTTTGACGGGTGTTTACCAGTCTATTACCTAGTTTTAACCCTGTTTCATATTCTACC AGAGTATAACAACCAATTAACCAATTCTGATTAG
U_S3-K220A-F	TGATGTAGCAACTGAAAATA
U_S3-K220A-R	TATTTTCAGTTGCTACATCA
U_S3EcoRVKan-F	GATC**GATATC**ATGGGACCATTGCCACTAAATCAAATAATTACGATAGAACGGGGTTTGCTAGGATGACGACGATAAGTAGGG
U_S3EcoRVKan-R	GATC**GATATC**CAACCAATTAACCAATTCTGATTAG
U_S3-F	TTATACTCTGGTAGAATATGAAACAGGGTTAAAACTAGGTAATAGACTGGATGTCTTCGAGTCCGGAGGC
U_S3FLAG-R	GCGTAGTATATATTATAAAATGAATCATTGAAGTTATTTTTGACGGGTGTTTACTTGTCGTCATCGTCTTTGTAGTCCAT ATGAGCGGCAGTTATCG

[a]The underlined sequences are homologs of pEPKan-S plasmid and were used to amplify the Kan^r gene cassette. The sequences in boldface are restriction enzyme sites.

analyses and ChIP-PCRs demonstrated that Meq and CREB are corecruited to the *LAT* and *meq* promoters (Fig. 5). Based on these results, we propose that one of the biological functions of MDV U_S3 is to ensure that those genomic regions are activated in the event that active cellular kinase signaling pathways are unavailable in the infected cells. Another interesting observation is that the interaction between Meq and U_S3 is phosphorylation dependent, indicating that additional proteins may be recruited to Meq by U_S3-mediated phosphorylation, facilitating the formation of a protein complex. This raises the interesting possibility that MDV U_S3 could trigger protein complex assembly, similar to what cellular ATR/ATM does (46). Although a previous study showed that CDK2 phosphorylation of Meq at serine 42 translocates Meq to the cytoplasm and decreases the DNA binding activity of Meq (47), we did not find that cotransfection of MDV U_S3 altered the subcellular localization of Meq (see Fig. S3), indicating that MDV U_S3 might target a serine/threonine residue different from that targeted by CDK2. Further studies are needed to map the U_S3 phosphorylation site of Meq and subsequent generation of Meq phosphorylation mutant viruses to explore the role of Meq phosphorylation in MDV pathogenesis and tumorigenesis. We suggest that viral kinases could play important roles in overriding key cellular signaling pathways to aid MDV replication. Taken together, our studies clearly demonstrated that one of the functions of MDV U_S3 is regulation of viral and cellular transcription through CREB activation.

MATERIALS AND METHODS

Cell culture. Primary CEF, prepared from 10- to 11-day-old chicken embryos, were grown in Leibowitz-McCoy (LM) (1:1) medium supplemented with 5% newborn calf serum at 37°C in the presence of 5% CO_2. DF-1, a chicken fibroblast line, and 293T, a human embryonic kidney epithelial cell line, were grown in Dulbecco's modified Eagle medium (DMEM) supplemented with 10% fetal bovine serum in the presence of 5% CO_2.

Mutagenesis of MDV 686-BAC. Deletion of the U_S3 gene from MDV 686-BAC was performed by two-step Red-mediated recombination as described previously (48). All the primers used for MDV 686-BAC mutagenesis are listed in Table 1. Briefly, the entire U_S3 ORF was first replaced with a kanamycin resistance (Kan^r) gene amplified from the plasmid pEPKan-S using primers U_S3-Kan-F and U_S3-Kan-R. Next, *the* Kan^r gene was deleted by inducing the expression of I-SceI by addition of 1% arabinose to the bacterial growth medium to generate 686-BACΔU_S3.

To generate 686-BAC-U_S3FLAG, the U_S3 ORF with a C-terminal FLAG tag was cloned into the pUC19 plasmid to generate pUC19-U_S3FLAG. To generate 686-BAC_U_S3-K220A, lysine (K) 220 of U_S3 was mutated to alanine (A) using primers U_S3-K220A-F and U_S3-K220A-R to generate pUC19-U_S3-K220A. Then, the Kan^r gene was amplified with primers U_S3EcoRVKan-F and U_S3EcoRVKan-R, with the pEPKan-S plasmid as the template. The amplified product was digested and cloned into the EcoRV site of pUC19-U_S3FLAG or pUC19-U_S3-K220A to generate pUC19-U_S3FLAG-Kan or pUC19-U_S3-K220A-Kan. Next, Us3-FLAG or U_S3-K220A with *the* Kan^r gene insertion was amplified with primers U_S3-F and U_S3FLAG-R to generate a Us3FLAG-Kan or U_S3-K220A-Kan transfer cassette, which was transfected by electroporation into competent cells carrying 686-BACΔU_S3 DNA to generate 686-BAC-U_S3FLAG or 686-BAC_U_S3-K220A. The BAC DNAs of 686-BACΔU_S3, 686-BAC-U_S3FLAG, and 686-BAC_U_S3-K220A were transfected into CEF by the calcium phosphate precipitation method to produce recombinant viruses.

Immunofluorescence assay. One day before transfection, 293T cells were seeded on coverslips placed in 6-well plates. The next day, pcDNA-HA-U_S3 or pcDNA-HA-U_S3-K220A plasmids were cotransfected, using polyethylenimine (PEI) (1 mg/ml), with the pcDNA-FLAG-Meq expression plasmid into 293T

cells. Forty-eight hours after transfection, the cells were fixed with 3.7% formaldehyde-phosphate-buffered saline (PBS) for 5 min at room temperature, followed by three washes with PBS. Then, the cells were permeabilized with 1.0% Triton X-100 and 1.0% NP-40 in PBS for 10 min each, followed by three washes with PBS. After blocking with 5% nonfat milk for 1 h at room temperature, the cells were incubated with mouse anti-hemagglutinin (HA) antibody and rabbit anti-FLAG antibody for 1 h, followed by another hour of incubation with goat anti-mouse-Texas Red and goat anti-rabbit-Alex Fluor 488 antibodies at room temperature. After three washes with PBS, the cells were stained with 4′, 6-diamidino-2-phenylindole (DAPI) for 5 min at room temperature. Cells on coverslips were mounted on glass slides with ProLong Diamond Antifade mountant and visualized with a Zeiss LSM 780 NLO multiphoton microscope.

Immunoprecipitation and Western blot assays. (i) IP with cell lysates isolated from 293T and DF-1 cells. 293T and DF-1 cells were seeded onto 60-mm plates 1 day before transfection with the indicated plasmids and PEI reagent. Forty-eight hours after transfection, the cells were lysed using EBC lysis buffer (50 mM Tris-HCl, 120 mM NaCl, 0.5% NP-40, 50 mM NaF, 200 μM Na_2VO_4, 1 mM phenylmethylsulfonyl fluoride) supplemented with protease inhibitors as described previously (49). The cell lysates (500 μg) were incubated with 25 μl of anti-FLAG agarose beads (Sigma) overnight at 4°C with gentle rotation. The next day, the agarose beads were washed five times with EBC lysis buffer and boiled for 5 min in 2× SDS loading buffer; 10% input control (50 μg cell lysates), together with immunoprecipitated samples, was applied for SDS-PAGE and transferred to polyvinylidene difluoride (PVDF) membranes (Millipore). The PVDF membranes were blocked with 5% nonfat milk in PBS containing 0.1% Tween 20 (PBST) for 1 h at room temperature, followed by incubation with primary antibody overnight at 4°C and horseradish peroxidase (HRP)-conjugated secondary antibodies for 1 h at room temperature. After three washes with PBST, the membranes were visualized with Super Signal West Pico Plus chemiluminescent substrate (Thermo Fisher Scientific) using the ChemiDocMP imaging system (Bio-Rad).

(ii) IP with cell lysates from recombinant 686-BAC-U_S3FLAG virus-infected CEF. Seven days after infection with recombinant virus, CEF were harvested for protein extraction with EBC lysis buffer supplemented with protease inhibitors. The cell lysates (500 μg) were incubated with 2 μg mouse anti-FLAG antibody (Sigma) or normal mouse IgG (Cell Signaling Technology) overnight at 4°C with gentle rotation. The next day, 25 μl of a protein A and protein G Sepharose bead (Invitrogen) mixture was added to the immune complex and rotated for 2 to 3 h at 4°C, followed by five washes with EBC lysis buffer, and then subjected to SDS-PAGE and WB analysis as described above. Quantification of WB band intensity was performed with Image J software.

Generation of recombinant baculoviruses and protein purification. *Spodoptera frugiperda* Sf9 cells were maintained in Ex-Cell 420 medium (Sigma). Recombinant baculoviruses expressing N-terminally FLAG-tagged U_S3, Meq, and pp38 were generated using the Bac-to-Bac baculovirus expression system (Invitrogen) according to the manufacturer's instructions. Briefly, the entire ORFs of U_S3, Meq, and pp38 were cloned into the pFastBac1-FLAG vector, followed by transformation of *Escherichia coli* DH10Bac to generate the recombinant bacmid. Recombinant bacmid DNA was transfected into Sf9 cells with PEI reagent to generate recombinant viruses. Protein expression was confirmed by WB with anti-FLAG antibody (Thermo Fisher Scientific). To produce and purify large amounts of proteins, 100 ml Sf9 cells was infected with recombinant baculovirus, which was harvested and lysed 2 days postinfection. Then, FLAG-tagged proteins were captured with anti-FLAG agarose beads (Sigma) and eluted with 3× FLAG peptide (Sigma), as described previously (49). The concentrations of purified proteins were measured with SDS-PAGE using bovine serum albumin (BSA) as a standard.

***In vitro* kinase assay.** An *in vitro* kinase assay was performed as described previously (49). Briefly, purified protein kinase (MDV U_S3) was incubated with purified substrates (MDV Meq or pp38) in kinase buffer supplemented with 10 μCi [γ-^{32}P]ATP at 37°C for 30 min. The reaction was stopped by adding 2× SDS loading buffer, and samples were then subjected to electrophoresis, followed by CBB staining. The gel was then dried and subjected to autoradiography.

RNA isolation and qRT-PCR. Transfected 293T or DF-1 cells and infected CEF were harvested for RNA isolation using TRIzol reagent (Invitrogen) according to the manufacturer's protocol. DNase I (Ambion) treatment was carried out after total RNA isolation, following the manufacturer's instructions. Total RNA (1 to 5 μg) from each sample was used for cDNA synthesis with oligo$(dT)_{12\text{-}18}$ primer (Invitrogen) using Moloney murine leukemia virus (MMLV) RT (Invitrogen). qRT-PCR was performed with the iCycler iQ real-time PCR detection system (Bio-Rad) using iTaq Universal SYBR green supermix (Bio-Rad). A melting curve analysis was performed to confirm the amplification of a single product. Experiments were repeated three times in triplicate. Gene expression was normalized to the GAPDH (glyceraldehyde-3-phosphate dehydrogenase) signal, and the qRT-PCR data were analyzed using the $2^{-\Delta\Delta CT}$ method (50).

Genomic-DNA isolation and MDV genome copy number. The extraction of genomic DNA from infected CEF was performed using a standard phenol-chloroform protocol, as previously described (51). The MDV genome copy number was determined by qPCR assay with primers specific to MDV *ICP4* and chicken *GAPDH* modified from a previously described protocol (52).

Dual-luciferase reporter assays. 293T cells were seeded on 12-well plates 1 day before transfection. The indicated plasmids were transfected together with reporter and *Renilla* luciferase vectors. Two days after transfection, firefly and *Renillla* luciferase activities were measured for each sample using the Dual-Glo luciferase assay system (Promega) according to the manufacturer's instructions. For data analysis, firefly luciferase data were normalized to *Renillla* luciferase activity, and fold changes were calculated by comparing the values generated with empty-vector-transfected cells. Experiments were

repeated three times in triplicate, and fold changes are shown as averages and standard errors of the mean (SEM).

ChIP and ChIP-seq analyses. ChIP assays were performed as described previously with minor modifications (24). Briefly, transfected 293T and DF-1 cells or infected CEF were fixed with 1% formaldehyde solution for 10 min at room temperature with gentle shaking and quenched with glycine. Chromatin was sheared using a Diagenode Bioruptor to an average size of about 300 bp and diluted 1:10, followed by incubation with antibody at 4°C overnight with gentle rotation; 1% of the diluted chromatin was collected to serve as an input control and stored at −20°C until it was used. The next day, the chromatin immunocomplexes were incubated with BSA-blocked magnetic protein A/G Dynabeads for 2 to 3 h at 4°C with gentle rotation. The chromatin immunocomplexes were then collected and washed four times. The immunoprecipitated chromatin was eluted in elution buffer by heating at 65°C for 30 min. The eluted chromatin and 1% input control were reverse cross-linked by incubation at 65°C overnight in the presence of 0.2 M sodium chloride (NaCl), followed by purification with a PCR purification kit (Qiagen) according to the manufacturer's instructions. PCR or qPCR analyses were performed in triplicate with input DNA (1:50 dilution) and ChIP DNA (1:5 dilution). ChIP enrichment signals were normalized to those derived from the input DNA control. The data represent averages and standard deviations of triplicates.

ChIP-seq analysis was performed as described previously (53). Briefly, chromatin DNA from 1×10^8 chicken T-cell lymphoma (SR8136) cells was used to precipitate Meq-bound chromatin with 10 μg of rabbit anti-Meq antibody. ChIP-enriched or input DNA was used to generate Illumina-compatible libraries with a Kapa LTO library preparation kit (Kapa Biosystems) according to the manufacturer's recommendations. The libraries were submitted for sequencing on an Illumina HiSeq 2500 sequencing system. The ChIP-seq data were aligned to Gullus_gullus-5.0 (GCA_000002315.3) of the chicken genome using the Bowtie 2 algorithm, and all the redundant tags were removed by the trimmomatic algorithm. Peak calling was performed using the MACS2 program with combined input as a reference set. The peak and read alignments were visualized using the Integrative Genomics Viewer (IGV) from the Broad Institute.

SUPPLEMENTAL MATERIAL

Supplemental material is available online only.

SUPPLEMENTAL FILE 1, PDF file, 5.3 MB.

ACKNOWLEDGMENTS

We thank Klaus Osterrieder for providing BAC reagents necessary for mutagenesis and Weston W. Porter for use of the Diagenode Bioruptor.

This work was supported by NIFA/AFRI/USDA grant 2014-67015-21787 and 2015-67015-23268, as well as TAMU CVM trainee grant 02-248020-18004.

REFERENCES

1. Osterrieder N, Kamil JP, Schumacher D, Tischer BK, Trapp S. 2006. Marek's disease virus: from miasma to model. Nat Rev Microbiol 4:283–294. https://doi.org/10.1038/nrmicro1382.
2. Cebrian J, Kaschka-Dierich C, Berthelot N, Sheldrick P. 1982. Inverted repeat nucleotide sequences in the genomes of Marek disease virus and the herpesvirus of the turkey. Proc Natl Acad Sci U S A 79:555–558. https://doi.org/10.1073/pnas.79.2.555.
3. Fukuchi K, Sudo M, Lee YS, Tanaka A, Nonoyama M. 1984. Structure of Marek's disease virus DNA: detailed restriction enzyme map. J Virol 51:102–109. https://doi.org/10.1128/JVI.51.1.102-109.1984.
4. Calnek BW. 2001. Pathogenesis of Marek's disease virus infection. Curr Top Microbiol Immunol 255:25–55.
5. Davison A. 2002. Comments on the phylogenetics and evolution of herpesviruses and other large DNA viruses. Virus Res 82:127–132. https://doi.org/10.1016/s0168-1702(01)00400-2.
6. Lee LF, Wu P, Sui D, Ren D, Kamil J, Kung HJ, Witter RL. 2000. The complete unique long sequence and the overall genomic organization of the GA strain of Marek's disease virus. Proc Natl Acad Sci U S A 97:6091–6096. https://doi.org/10.1073/pnas.97.11.6091.
7. Tulman ER, Afonso CL, Lu Z, Zsak L, Rock DL, Kutish GF. 2000. The genome of a very virulent Marek's disease virus. J Virol 74:7980–7988. https://doi.org/10.1128/jvi.74.17.7980-7988.2000.
8. Lupiani B, Lee LF, Cui X, Gimeno I, Anderson A, Morgan RW, Silva RF, Witter RL, Kung HJ, Reddy SM. 2004. Marek's disease virus-encoded Meq gene is involved in transformation of lymphocytes but is dispensable for replication. Proc Natl Acad Sci U S A 101:11815–11820. https://doi.org/10.1073/pnas.0404508101.
9. Trapp S, Parcells MS, Kamil JP, Schumacher D, Tischer BK, Kumar PM, Nair VK, Osterrieder N. 2006. A virus-encoded telomerase RNA promotes malignant T cell lymphomagenesis. J Exp Med 203:1307–1317. https://doi.org/10.1084/jem.20052240.
10. Deruelle MJ, Favoreel HW. 2011. Keep it in the subfamily: the conserved alphaherpesvirus US3 protein kinase. J Gen Virol 92:18–30. https://doi.org/10.1099/vir.0.025593-0.
11. Wang X, Patenode C, Roizman B. 2011. US3 protein kinase of HSV-1 cycles between the cytoplasm and nucleus and interacts with programmed cell death protein 4 (PDCD4) to block apoptosis. Proc Natl Acad Sci U S A 108:14632–14636. https://doi.org/10.1073/pnas.1111942108.
12. Kato A, Arii J, Shiratori I, Akashi H, Arase H, Kawaguchi Y. 2009. Herpes simplex virus 1 protein kinase Us3 phosphorylates viral envelope glycoprotein B and regulates its expression on the cell surface. J Virol 83:250–261. https://doi.org/10.1128/JVI.01451-08.
13. Kato A, Yamamoto M, Ohno T, Tanaka M, Sata T, Nishiyama Y, Kawaguchi Y. 2006. Herpes simplex virus 1-encoded protein kinase UL13 phosphorylates viral Us3 protein kinase and regulates nuclear localization of viral envelopment factors UL34 and UL31. J Virol 80:1476–1486. https://doi.org/10.1128/JVI.80.3.1476-1486.2006.
14. Walters MS, Kinchington PR, Banfield BW, Silverstein S. 2010. Hyperphosphorylation of histone deacetylase 2 by alphaherpesvirus US3 kinases. J Virol 84:9666–9676. https://doi.org/10.1128/JVI.00981-10.
15. Wang K, Ni L, Wang S, Zheng C. 2014. Herpes simplex virus 1 protein kinase US3 hyperphosphorylates p65/RelA and dampens NF-kappaB activation. J Virol 88:7941–7951. https://doi.org/10.1128/JVI.03394-13.
16. Wu H, Li T, Zeng M, Peng T. 2012. Herpes simplex virus type 1 infection activates the Epstein-Barr virus replicative cycle via a CREB-dependent mechanism. Cell Microbiol 14:546–559. https://doi.org/10.1111/j.1462-5822.2011.01740.x.
17. Schumacher D, Tischer BK, Trapp S, Osterrieder N. 2005. The protein encoded by the US3 orthologue of Marek's disease virus is required for efficient de-envelopment of perinuclear virions and involved in actin stress fiber breakdown. J Virol 79:3987–3997. https://doi.org/10.1128/JVI.79.7.3987-3997.2005.

18. Schumacher D, McKinney C, Kaufer BB, Osterrieder N. 2008. Enzymatically inactive U(S)3 protein kinase of Marek's disease virus (MDV) is capable of depolymerizing F-actin but results in accumulation of virions in perinuclear invaginations and reduced virus growth. Virology 375:37–47. https://doi.org/10.1016/j.virol.2008.01.026.
19. Benetti L, Roizman B. 2004. Herpes simplex virus protein kinase US3 activates and functionally overlaps protein kinase A to block apoptosis. Proc Natl Acad Sci U S A 101:9411–9416. https://doi.org/10.1073/pnas.0403160101.
20. Jones D, Lee L, Liu JL, Kung HJ, Tillotson JK. 1992. Marek disease virus encodes a basic-leucine zipper gene resembling the fos/jun oncogenes that is highly expressed in lymphoblastoid tumors. Proc Natl Acad Sci U S A 89:4042–4046. https://doi.org/10.1073/pnas.89.9.4042.
21. Suchodolski PF, Izumiya Y, Lupiani B, Ajithdoss DK, Gilad O, Lee LF, Kung HJ, Reddy SM. 2009. Homodimerization of Marek's disease virus-encoded Meq protein is not sufficient for transformation of lymphocytes in chickens. J Virol 83:859–869. https://doi.org/10.1128/JVI.01630-08.
22. Suchodolski PF, Izumiya Y, Lupiani B, Ajithdoss DK, Lee LF, Kung HJ, Reddy SM. 2010. Both homo and heterodimers of Marek's disease virus encoded Meq protein contribute to transformation of lymphocytes in chickens. Virology 399:312–321. https://doi.org/10.1016/j.virol.2010.01.006.
23. Brown AC, Smith LP, Kgosana L, Baigent SJ, Nair V, Allday MJ. 2009. Homodimerization of the Meq viral oncoprotein is necessary for induction of T-cell lymphoma by Marek's disease virus. J Virol 83:11142–11151. https://doi.org/10.1128/JVI.01393-09.
24. Levy AM, Izumiya Y, Brunovskis P, Xia L, Parcells MS, Reddy SM, Lee L, Chen HW, Kung HJ. 2003. Characterization of the chromosomal binding sites and dimerization partners of the viral oncoprotein Meq in Marek's disease virus-transformed T cells. J Virol 77:12841–12851. https://doi.org/10.1128/jvi.77.23.12841-12851.2003.
25. Subramaniam S, Johnston J, Preeyanon L, Brown CT, Kung HJ, Cheng HH. 2013. Integrated analyses of genome-wide DNA occupancy and expression profiling identify key genes and pathways involved in cellular transformation by a Marek's disease virus oncoprotein, Meq. J Virol 87:9016–9029. https://doi.org/10.1128/JVI.01163-13.
26. Carlezon WA, Jr, Duman RS, Nestler EJ. 2005. The many faces of CREB. Trends Neurosci 28:436–445. https://doi.org/10.1016/j.tins.2005.06.005.
27. Wu X, Spiro C, Owen WG, McMurray CT. 1998. cAMP response element-binding protein monomers cooperatively assemble to form dimers on DNA. J Biol Chem 273:20820–20827. https://doi.org/10.1074/jbc.273.33.20820.
28. Mayr B, Montminy M. 2001. Transcriptional regulation by the phosphorylation-dependent factor CREB. Nat Rev Mol Cell Biol 2:599–609. https://doi.org/10.1038/35085068.
29. Sharma-Walia N, George Paul A, Patel K, Chandran K, Ahmad W, Chandran B. 2010. NFAT and CREB regulate Kaposi's sarcoma-associated herpesvirus-induced cyclooxygenase 2 (COX-2). J Virol 84:12733–12753. https://doi.org/10.1128/JVI.01065-10.
30. Francois S, Sen N, Mitton B, Xiao X, Sakamoto KM, Arvin A. 2016. Varicella-zoster virus activates CREB, and inhibition of the pCREB-p300/CBP interaction inhibits viral replication in vitro and skin pathogenesis in vivo. J Virol 90:8686–8697. https://doi.org/10.1128/JVI.00920-16.
31. Lu F, Zhou J, Wiedmer A, Madden K, Yuan Y, Lieberman PM. 2003. Chromatin remodeling of the Kaposi's sarcoma-associated herpesvirus ORF50 promoter correlates with reactivation from latency. J Virol 77:11425–11435. https://doi.org/10.1128/jvi.77.21.11425-11435.2003.
32. Du T, Zhou G, Roizman B. 2013. Modulation of reactivation of latent herpes simplex virus 1 in ganglionic organ cultures by p300/CBP and STAT3. Proc Natl Acad Sci U S A 110:E2621–E2628. https://doi.org/10.1073/pnas.1309906110.
33. de Oliveira PS, Ferraz FA, Pena DA, Pramio DT, Morais FA, Schechtman D. 2016. Revisiting protein kinase-substrate interactions: toward therapeutic development. Sci Signal 9:re3. https://doi.org/10.1126/scisignal.aad4016.
34. Kim J, Li G, Walters MA, Taylor SS, Veglia G. 2016. Uncoupling catalytic and binding functions in the cyclic AMP-dependent protein kinase A. Structure 24:353–363. https://doi.org/10.1016/j.str.2015.11.016.
35. Chan JY, Chen WC, Lee HY, Chang TJ, Chan SH. 1999. Phosphorylation of transcription factor cyclic-AMP response element binding protein mediates c-fos induction elicited by sustained hypertension in rat nucleus tractus solitarii. Neuroscience 88:1199–1212. https://doi.org/10.1016/s0306-4522(98)00273-5.
36. Haque R, Chong NW, Ali F, Chaurasia SS, Sengupta T, Chun E, Howell JC, Klein DC, Iuvone PM. 2011. Melatonin synthesis in retina: cAMP-dependent transcriptional regulation of chicken arylalkylamine N-acetyltransferase by a CRE-like sequence and a TTATT repeat motif in the proximal promoter. J Neurochem 119:6–17. https://doi.org/10.1111/j.1471-4159.2011.07397.x.
37. Cha-Molstad H, Keller DM, Yochum GS, Impey S, Goodman RH. 2004. Cell-type-specific binding of the transcription factor CREB to the cAMP-response element. Proc Natl Acad Sci U S A 101:13572–13577. https://doi.org/10.1073/pnas.0405587101.
38. Kato A, Yamamoto M, Ohno T, Kodaira H, Nishiyama Y, Kawaguchi Y. 2005. Identification of proteins phosphorylated directly by the Us3 protein kinase encoded by herpes simplex virus 1. J Virol 79:9325–9331. https://doi.org/10.1128/JVI.79.14.9325-9331.2005.
39. Erazo A, Kinchington PR. 2010. Varicella-zoster virus open reading frame 66 protein kinase and its relationship to alphaherpesvirus US3 kinases. Curr Top Microbiol Immunol 342:79–98. https://doi.org/10.1007/82_2009_7.
40. Singh V, Ram M, Kumar R, Prasad R, Roy BK, Singh KK. 2017. Phosphorylation: implications in cancer. Protein J 36:1–6. https://doi.org/10.1007/s10930-017-9696-z.
41. Kato A, Tsuda S, Liu Z, Kozuka-Hata H, Oyama M, Kawaguchi Y. 2014. Herpes simplex virus 1 protein kinase Us3 phosphorylates viral dUTPase and regulates its catalytic activity in infected cells. J Virol 88:655–666. https://doi.org/10.1128/JVI.02710-13.
42. Xiong R, Rao P, Kim S, Li M, Wen X, Yuan W. 2015. Herpes simplex virus 1 US3 phosphorylates cellular KIF3A to downregulate CD1d expression. J Virol 89:6646–6655. https://doi.org/10.1128/JVI.00214-15.
43. Wang S, Wang K, Lin R, Zheng C. 2013. Herpes simplex virus 1 serine/threonine kinase US3 hyperphosphorylates IRF3 and inhibits beta interferon production. J Virol 87:12814–12827. https://doi.org/10.1128/JVI.02355-13.
44. Delghandi MP, Johannessen M, Moens U. 2005. The cAMP signalling pathway activates CREB through PKA, p38 and MSK1 in NIH 3T3 cells. Cell Signal 17:1343–1351. https://doi.org/10.1016/j.cellsig.2005.02.003.
45. Everett LJ, Le Lay J, Lukovac S, Bernstein D, Steger DJ, Lazar MA, Kaestner KH. 2013. Integrative genomic analysis of CREB defines a critical role for transcription factor networks in mediating the fed/fasted switch in liver. BMC Genomics 14:337. https://doi.org/10.1186/1471-2164-14-337.
46. Marechal A, Zou L. 2013. DNA damage sensing by the ATM and ATR kinases. Cold Spring Harb Perspect Biol 5:a012716. https://doi.org/10.1101/cshperspect.a012716.
47. Liu JL, Ye Y, Qian Z, Qian Y, Templeton DJ, Lee LF, Kung HJ. 1999. Functional interactions between herpesvirus oncoprotein MEQ and cell cycle regulator CDK2. J Virol 73:4208–4219. https://doi.org/10.1128/JVI.73.5.4208-4219.1999.
48. Tischer BK, von Einem J, Kaufer B, Osterrieder N. 2006. Two-step red-mediated recombination for versatile high-efficiency markerless DNA manipulation in Escherichia coli. Biotechniques 40:191–197. https://doi.org/10.2144/000112096.
49. Izumiya Y, Izumiya C, Van Geelen A, Wang DH, Lam KS, Luciw PA, Kung HJ. 2007. Kaposi's sarcoma-associated herpesvirus-encoded protein kinase and its interaction with K-bZIP. J Virol 81:1072–1082. https://doi.org/10.1128/JVI.01473-06.
50. Nakayama K. 2013. cAMP-response element-binding protein (CREB) and NF-kappaB transcription factors are activated during prolonged hypoxia and cooperatively regulate the induction of matrix metalloproteinase MMP1. J Biol Chem 288:22584–22595. https://doi.org/10.1074/jbc.M112.421636.
51. Silva RF, Reddy SM, Lupiani B. 2004. Expansion of a unique region in the Marek's disease virus genome occurs concomitantly with attenuation but is not sufficient to cause attenuation. J Virol 78:733–740. https://doi.org/10.1128/jvi.78.2.733-740.2004.
52. Heidari M, Delekta PC. 2017. Transcriptomic analysis of host immune response in the skin of chickens infected with Marek's disease virus. Viral Immunol 30:377–387. https://doi.org/10.1089/vim.2016.0172.
53. Lyu Y, Nakano K, Davis RR, Tepper CG, Campbell M, Izumiya Y. 2017. ZIC2 is essential for maintenance of latency and is a target of an immediate early protein during Kaposi's sarcoma-associated herpesvirus lytic reactivation. J Virol 91:e00980-17. https://doi.org/10.1128/JVI.00980-17.